SIMULTANEOUS PIV AND LIF EXPERIMENTS ON A ROUND JET IN COUNTERFLOW

Stefano Bernero
Heinrich E. Fiedler
Hermann-Föttinger-Institut für Strömungsmechanik
Technische Universität Berlin
Str. des 17. Juni 135, 10623 Berlin, Germany

ABSTRACT

In the present work Particle-image-velocimetry (PIV) and Laser-induced-fluorescence (LIF) have been simultaneously applied to the study of a round jet in a counterflowing stream. The aim of the study was, on one side, the investigation of the potentiality and the limits of this newly developed technique. On the other side, it was attempted to combine the information obtained with the two methods in order to contribute to the understanding of this complex flow phenomenon.

Instantaneous LIF images show a good correspondence with the vorticity structures obtained from PIV. By comparing the statistics of the results from the two methods a general agreement is observed, which however not always holds also in detail, and a relationship is proposed between concentration and velocity field.

NOMENCLATURE

- b Half-velocity width (at $(U+U_0)/(U_j+U_0)=0.5$)
- b_c Half-concentration width (at $C/C_j=0.5$)
- x Axial coordinate
- x_p Average penetration length
- y Radial coordinate (axisymmetric coord. system)
- C Time averaged concentration
- C_j Initial concentration (at jet exit)
- Q Total volume flux ($=\int_0^{y^*} 2\pi y u\, dy$)
- U Time averaged axial velocity
- U_j Jet exit velocity
- U_0 Counterflow velocity
- α Jet-to-counterflow velocity ratio ($=U_j/U_0$)

INTRODUCTION

PIV and LIF have recently become more and more important in the experimental investigation of turbulent flow phenomena. Given their compatibility, the next step is now the combination of LIF and PIV to yield simultaneous information on both vector (velocity) and scalar (concentration) field.

A method for simultaneous LIF and PIV imaging with the use of two synchronized cameras and a scanner system was newly developed in this institute (Taubert, 1997) and is here applied to the study of an axisymmetrical jet issuing into a uniform stream with opposite direction. The present study has therefore the twofold purpose of testing the technique on a different and quite challenging case as well as of obtaining new information about this interesting but scarcely understood flow.

The lack of knowledge on the mechanics of the jet in counterflow can be mostly explained by its strong instability, which hinders both the experimental approach and the theoretical interpretation of the phenomenon. Instead it is clear that jet mixing is enhanced by the counterflow (Beltaos and Rajaratnam, 1973; Yoda and Fiedler, 1996; Bernero and Fiedler, 1998), therefore a further understanding of this flow would be of interest for engineering applications, which could be found in combustion or mixing processes in general, both in technology and in the environment.

A jet in counterflow shows in its near field a behavior which is similar to that of a jet issuing in a stagnant ambient when the reduction of the potential core length, corresponding to the "compression" of the jet column by the counterflow, is taken into account. In

the far field, instead, the jet tip interacts with the counterflowing stream, by which it is deflected to one side and, with further dilution, convected backwards. The orientation and amplitude of the jet deflection are not fixed, whereby the jet tip appears to oscillate with low frequency (Yoda and Fiedler, 1996) around the axis and on planes across the axis. No particular pattern could be found for these fluctuations, even through visualizations in radial planes of the jet (Bernero, 1998), but they are generally not biased, so that time averaged results appear to be symmetric. Statistical data can therefore be obtained and compared with those of a free jet; further information on the dynamics of the flow, however, can be gained only from the instantaneous flowfields, which are instead strongly asymmetric and unstable.

Both the faster axial decay due to the "compression" of the jet column and the stirring generated by the oscillations of the jet tip contribute to increase the mixing efficiency of a jet in counterflow. A better understanding of this feature, in view of its further enhancement and control, would therefore be relevant for possible practical applications.

EXPERIMENTAL SETUP AND PROCEDURES

Experiments were carried out in a water tunnel with square, 30 *cm* wide, vertical cross-section at a fixed counterflow velocity of 13 cm/s. The jet was fed through nozzles with fifth order polynomial inner contour and exit diameter D of 10, 5, and 2 *mm*, which were used alternatively to generate jet-to-counterflow velocity ratios ranging from 1.3 to 20 while keeping the effect of the wall channels negligible. The jet had flat-top exit profiles and the counterflow had a uniform profile with a background turbulence level of about 1.6%.

A sketch of the measurement system is shown in Figure 1. The basic optical and electronic equipment and the methodology were the same as described in (Taubert, 1997): the beam of a 5 W Argon-ion laser was scanned through the axial plane of the jet and the images were captured by two CCD cameras, recorded on tape, and then digitized through a frame grabber. The cameras were synchronized with the scanners to obtain two exposures corresponding to the two half-frames of every video image. The time interval between the two exposures Δt could be adjusted up to a minimum of 2.4 *ms*, which is the value used in the present experiments. Rhodamine 6G was added to the jet fluid and VESTOSINT particles with a diameter of 20 μm were used as tracer for PIV.

A color filter placed in front of the LIF camera was able to remove virtually all the PIV particles from the LIF-image (Figure 2). Differently from (Taubert, 1997),

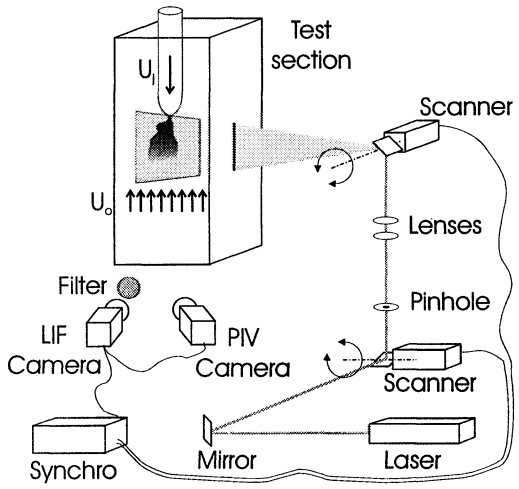

Figure 1. Experimental setup.

here no filter was used for the PIV camera, otherwise the particle density in the image would have been reduced too drastically. The fluorescence in the background, however, seemed not to affect the quality of the PIV results or to increase the number of outliers. Also, here no further image enhancement was required after digitalization. Both differences in the procedure can be explained by the fact that in the present case the size of the measuring area was much larger than in (Taubert, 1997) so that the particle images appeared less bright, but at the same time also the undesired side-effect of light scattering was reduced.

PIV displacements were calculated through cross-correlation with a program based on PIVWARE (Westerveel, 1993) and further extended in this institute to improve the accuracy through a window shifting procedure (Blümel and Taubert, 1996). The chosen window size of 32x32 pixels with 50% overlapping in each direction corresponded, with an image size of about 90x68 *mm* and a CCD size of 768x576 pixels, to a spatial resolution of about 2 *mm*. The actual pixel size, which corresponds to the spatial resolution of LIF, was therefore about 0.12 *mm*. The exact scaling of the images, as well as the correspondence between the areas captured by the two cameras, was made possible by acquiring images of a fixed reference frame positioned on the axial plane of the jet before each experimental run. The concentration of fluorescent dye ($2.5 \cdot 10^{-7} mol/l$) was low enough to be in the range where linear dependence exists between fluorescence intensity ($\simeq$ gray value of digitized image) and concentration. Calibration of LIF images could then be performed to obtain concentration, using images of the counterflow alone with a small and uniform dye concentration as a reference.

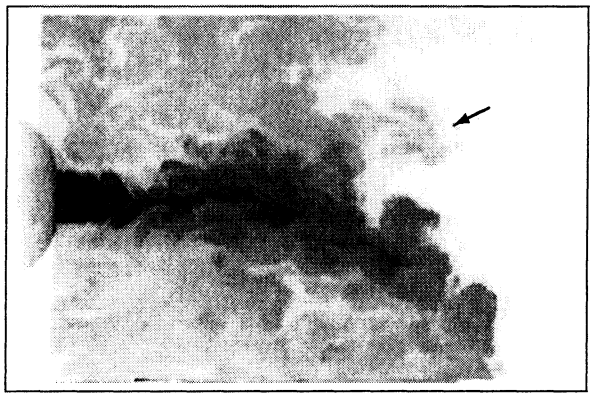

Figure 2. Instantaneous LIF image at a jet-to-counterflow velocity ratio of 3.4 with D=10 mm.

Figure 3. Instantaneous PIV/LIF image: superposition of Figure 2 and corresponding PIV vorticity contours.

RESULTS AND DISCUSSION

Some general results about the jet in counterflow obtained in the present channel with the use of LDA and LIF were reported in (Yoda and Fiedler, 1996; Bernero and Fiedler, 1998). Here we shall discuss the possibility of application of the simultaneous PIV/LIF technique to this flow and present some of the results obtained so far.

Limitations are mostly related to the spatial and temporal resolution of PIV. Given the limited number of pixels in the CCD and the size of the total flowfield, large velocity gradients cannot be resolved. This appears, e.g., in the shear layer (see Figure 3, where the vorticity contours can help identify areas of concentrated positive and negative vorticity but cannot resolve the single vortex rings). The errors are even larger in the case of the 2 *mm* nozzle with the higher velocity ratios: here, in proximity of the jet axis, the particle displacement and the pattern distortion within the interrogation windows are so large that the gradients and the velocity maximum on the axis are leveled off. The values of velocity on the axis, therefore, cannot be considered representative for $x < 0.75x_p$ (see Figure 10).

These errors could be of course reduced by limiting the extension of the imaged area to the near field, but it is important to include also the far field if we want to follow the larger flow structures and to determine the external boundaries of the mixing region in order to calculate its extension. Time resolution, due to the fixed 25 Hz video frequency, is anyway not sufficient to follow in successive time steps the smaller and faster structures which appear in the near field. Instead, as they travel downstream and they are slowed down and deflected backwards by the counterflow, some structures can be individually followed in their motion. This can be done at best with PIV, which allows to identify vorticity structures also after the ones from LIF have already been smoothed out by diffusion.

Further improvements, especially in the near field and for the case of high velocity ratios, might also be achieved by reducing the time interval between the two exposures. This is however quite demanding, since it would involve either changing the scanner system or, better, shifting to a system with two pulsed YAG lasers, where Δt could be arbitrarily adjusted.

The superposition of an instantaneous LIF-image and the corresponding vorticity contours calculated from PIV (Figure 3) shows that the flow visualization corresponds quite well with the vorticity structures. The "mushroom" vortex that appears in the picture (see arrow in Figure 2) is a typical heritage of the jet tip wandering and shows that occasionally also couples of counter-rotating vortices can be swept back together on one side of the jet axis. Normally, instead, only outwards-rotating vortices can be seen on each side of the jet.

A series of 400 images was acquired for each experiment for calculating some statistics on the flow. Even though this number might be too low for a complete statistical study, it seemed to be a reasonable compromise between the time and memory requirements for image processing and the need of accuracy, especially taking into account that no higher-order moments are calculated, but only averages and rms values. The time records for the simultaneous PIV/LIF experiments had a length of 96 s, so that the sampling frequency resulted to be around 4.2 Hz. In order to increase the number of test cases and perform some comparisons, some images from separate PIV and LIF experiments were evaluated as well. In these cases the time records were twice as long, yielding a sampling frequency of about 2.1 Hz

At this point it must be mentioned that for considerations on the statistics of the flow there is no need for the

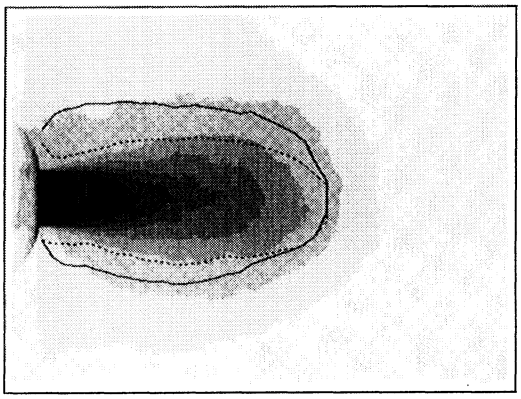

Figure 4. Average of the LIF gray values together with two dividing streamlines calculated from PIV (– – U=0, —— stagnation stream surface, i.e. Q=0); α=2.2 and D=10 mm.

Figure 5. RMS of the LIF gray values with superimposed contours of the rms of U-velocity fluctuations from PIV; α=2.2 and D=10 mm.

PIV and LIF experiments to be performed simultaneously. Nevertheless, due to the strong instability and the sensitivity of the flow to even small angles between jet and counterflow (Yoda and Fiedler, 1996), it is preferable that also some series of simultaneous experiments be available, at least as a reference and in order to be sure that no other factors can affect the comparison between the results from the two methods.

A qualitative comparison between statistics from simultaneous LIF and PIV data is shown in Figures 4 and 5 for the sample case of $\alpha = 2.2$. In both figures the LIF results are represented by gray levels, whose number was reduced to 10 for simplicity. From Figure 4 it can be seen that the dividing lines calculated from PIV have a shape that does not correspond to the one of the LIF contours, but lie within the 20% and the 30% concentration boundary. The rms values from PIV (Figure 5) confirm the assumption (Bernero and Fiedler, 1998) that two regions of high mixing are present, one in the shear layer and the other where the velocity inversion takes place, with large radial fluctuations of the jet.

Since the most interesting feature of the jet in counterflow for practical applications is its mixing efficiency, which is able to produce a rather uniform mixture of jet and counterflow fluid within a limited region, it is of fundamental importance to define the boundaries of this mixing region. Almost all studies available in literature agree over the axial extension of the mixing region and propose a linear relationship between average penetration length x_p and jet-to-counterflow velocity ratio α. Over the radial boundary of the mixing region there are instead some contrasting data, also because different methods are used for defining and calculating it.

In the following some results from the analysis of the average flowfield are presented, aimed at defining the extension of the mixing region more univocally, through the combined use of PIV and LIF, as well as at a general quantitative comparison between these two methods.

When the velocity field is available, both the dividing streamline $U = 0$ and the stagnation stream surface, over which the total volume flux Q is zero, can be easily defined and the latter can be taken as the significant boundary. On the contrary, the definition for measurements of the concentration field (or for uncalibrated flow visualizations) is not so straightforward and a fixed percentage of the initial gray value is usually taken as a threshold (Yoda and Fiedler, 1996; Lam and Chan, 1997). Here it is suggested to use, instead, the fraction $1/(1+\alpha)$ of the initial gray value, since this corresponds to the point $U = 0$ in the centerline velocity decay when this is normalized to the range [0,1]. If the penetration length is calculated from PIV and this x_p value is then used to check the corresponding percentage in the centerline concentration decay, the points shown on Figure 6 are obtained. It can be seen that these points do not fall exactly on the $1/(1+\alpha)$ curve, still the curve represents their behavior much better than how a fixed percentage value would do. For high values of α, though, the slope decreases and a fixed value between 5% and 10% might be acceptable.

The points in which the concentration C falls to $1/(1+\alpha)$ of its initial value C_j can therefore be assumed to be equivalent to the dividing streamline $U = 0$. By integrating the concentration along y as done with velocity for the total volume flux (with the concentrations at radial positions outside the above defined dividing streamline taken as negative), a line equivalent to the $Q = 0$ should be obtained. The separating lines calculated with the above methods are shown in Figure 7 for a few sample cases: the penetration length is smaller

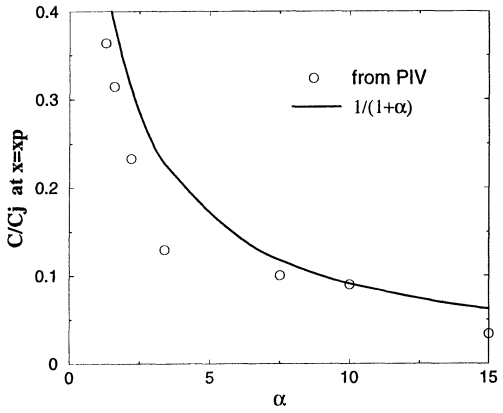

Figure 6. Fraction of initial concentration value at $x = x_p$.

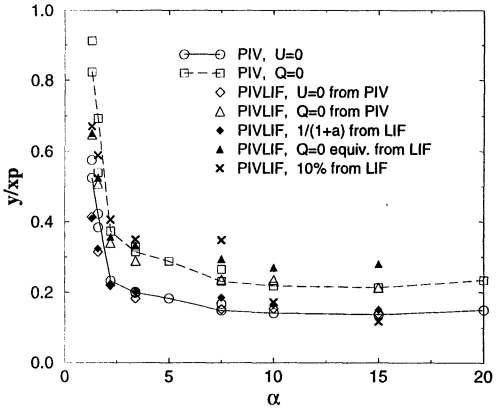

Figure 8. Maximum radial extension of mixing region.

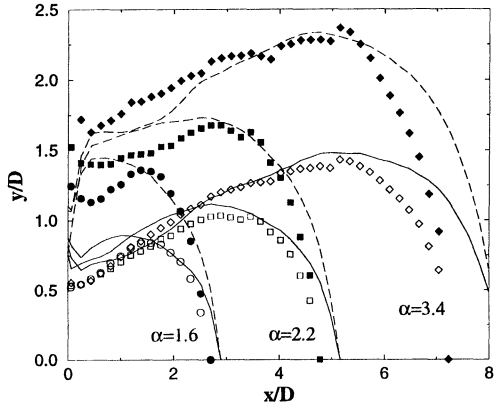

Figure 7. Boundaries of the mixing region from simultaneous PIV (—— U=0 and – – Q=0) and LIF (empty and filled symbols: lines corresponding to U=0 and Q=0, respectively).

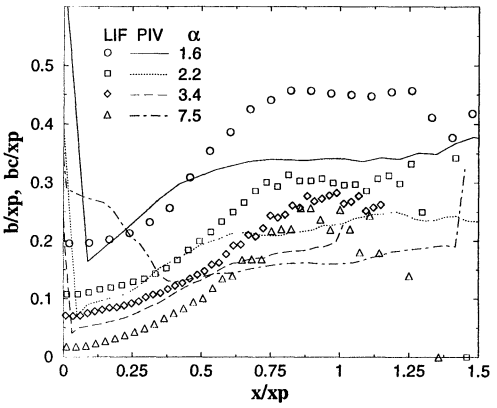

Figure 9. Half-velocity and half-concentration width.

for LIF than for PIV, but the shape of the curves and the radial extension appear to be similar for both methods.

The maximum half-width of these separating lines, which is usually taken as a parameter to characterize the radial extension of the mixing region, is shown in Figure 8. Again there is good agreement between the PIV and the LIF values calculated with the above method. Here also the values calculated from LIF with a fixed 10% limit are presented, and in all cases the width decreases with α. While the data from LIF show a more irregular trend, the values from PIV assume an almost constant value above $\alpha = 7.5$, which corresponds to about $0.14x_p$ for the $U = 0$ boundary and about $0.22x_p$ for the $Q = 0$ one.

The growth rate of a jet is usually calculated as the slope of the line representing the half-velocity width b after the jet has reached self-similarity. In the case of a jet in counterflow the self-similarity is never achieved totally (see below), but still b can be used to estimate the growth rate and therefore to evaluate the effect of the counterflow on jet spreading. In the present case both the half-velocity width b and the half-concentration width b_c were calculated and some of the curves obtained are presented in Figure 9. It appears that the widths obtained from LIF are larger than the ones from PIV, as shown also by the slope of the curves, which lies between 0.2 and 0.4 for LIF and between 0.1 and 0.2 for PIV. Both ranges are, however, above the value of the growth rate for a jet in quiescent ambient (= 0.1), and this can be taken as a measure of the mixing enhancement produced by the counterflow.

Normalized profiles of the centerline velocity and the centerline concentration decay are shown in Figure 10. It can be noticed that there are some irregularities in the correspondence between LIF and PIV data, but the behavior is similar, so that LIF might be used to estimate also the velocity profiles in the case of high α-values, where PIV fails to yield correct data in the near field. The axial profiles of the rms values of velocity and concentration also show similarity between PIV and LIF re-

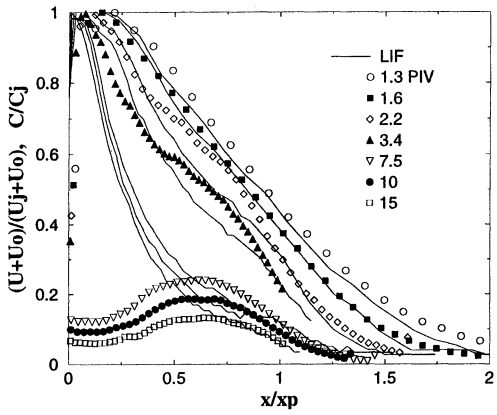

Figure 10. Normalized profiles of centerline velocity decay and centerline concentration decay.

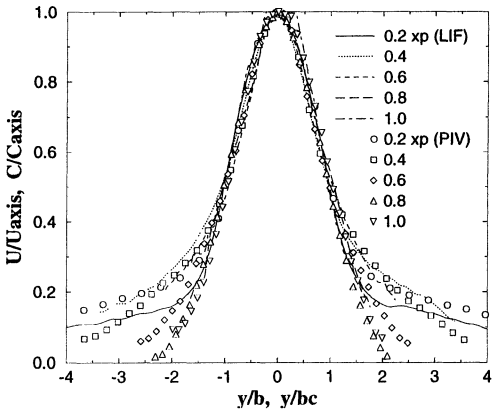

Figure 11. Self-similarity of velocity and concentration profiles; α=3.4 and D=10 mm.

sults, but only qualitatively. As seen in Figure 5, the rms values grow to a maximum at the end of the potential core, then decay showing another relative maximum in proximity of x_p. Both maxima seem more pronounced and appear at higher x-values for LIF than for PIV.

An example of radial velocity and concentration profiles normalized for verifying self similarity is shown in Figure 11. The present results, both from PIV and from LIF, confirm the observation (Yoda and Fiedler, 1996; Bernero and Fiedler, 1998) that a region of jet-like self-similarity exists near the axis, while in the external region the profiles are not self-similar.

CONCLUSIONS

The upgrading of a PIV system with simultaneous LIF involves no major changes to the setup and, in the present case, also no losses in the quality of PIV data. LIF and PIV results show a good agreement in general, even if not always in detail. With the proposed relationship between concentration and velocity profiles, however, the extension of the mixing region calculated from the two methods is approximately the same.

Some observations made with LIF data, which are easier to obtain, can also be extended to the velocity field, with the additional advantage that LIF yields a better spatial resolution and also allows to obtain reasonable data in regions where gradients are high. On the other hand, for a quantitative description of the flow, PIV is more reliable since it does not need a calibration and is more accurate at the external boundary of the flow, where LIF suffers from discretization due to the limited number of available gray values.

Simultaneous PIV and LIF experiments seem therefore to be a precious help in collecting complete data for the analysis of the flow and for the understanding of its dynamics.

ACKNOWLEDGMENT

The project was sponsored by DAAD (German Academic Exchange Program), the Rotary Foundation, and the European Commission, TMR Program, contract no. ERBFMBICT97-1915.

REFERENCES

Beltaos S., Rajaratnam N. , 1973, "Circular Turbulent Jet in an Opposing Infinite Stream", *Proc. 1st Can. Hydr. Conf.*, Edmonton, pp.220–237.

Bernero, S., 1998, "Der Freistrahl im Gegenstrom", Institute report 1997-98, HFI/TU Berlin.

Bernero, S. and Fiedler, H.E., 1998, "Experimental Investigations of a Jet in Counterflow, *Advances in Turbulence 7*, Frisch ed., Kluwer, Amsterdam, pp. 35–38.

Blümel, B. and Taubert, L., 1996, "Untersuchung des Mischverhaltens in duesennahen Freistrahl bei Beeinflussung von Wirbeldynamik und -zerfall", Institute report 1995-96, HFI/TU Berlin.

Lam K.M. and Chan H.C., 1997, "Round Jet in Ambient Counterflowing Stream, *ASCE Journ. of Hydr. Eng.*, 123. No. 10, pp.1–8.

Taubert, L., 1997, "Verknüpfung von LIF und PIV – Messungen an einem Freistrahl hoher Schmidtzahl", Diplom Thesis, HFI/TU Berlin.

Westerveel, J., 1993, "Digital Particle Image Velocimetry - Theory and Application", Ph.D. Thesis, TU Delft.

Yoda, M. and Fiedler, H.E., 1996, "The Round Jet in a Uniform Counterflow: Flow Visualization and Mean Concentration Measurements", *Expts. in Fluids* , Vol. 21, pp. 427–436.